

Satellite Article

Magnetic resonance imaging of the distal limb of the standing horse

T. S. MAIR*, J. KINNS, R. D. JONES AND N. M. BOLAS

Bell Equine Veterinary Clinic, Mereworth, Maidstone, Kent ME18 5GS, UK.

Keywords: horse; distal limb; orthopaedics; MRI

Introduction

Magnetic resonance imaging (MRI) is a new and potentially very useful imaging modality in equine orthopaedics. In MRI, the part of the limb being imaged is placed within a strong magnetic field and subjected to perturbing radiofrequency (RF), pulses. A unique RF signal, based on each tissue's magnetic characteristics, is emitted in response to the perturbing pulses, and these RF pulses are collected to form the image (Kraft and Gavin 2001; Tucker and Sande 2001). Magnetic resonance signal intensity varies widely in different musculoskeletal tissues, due to differences in proton density and status of the chemically free vs. bound molecular water (Kraft and Gavin 2001). The high soft tissue contrast afforded by MRI makes it ideal for assessment of articular cartilage, ligaments, tendons, joint capsules, synovium and bone marrow (Buckwalter 1996; Widmer *et al.* 1999). Magnetic resonance imaging has proved to be extremely valuable in the evaluation of the musculoskeletal system in man, and it has now become the technique of choice to investigate many structures including the knee (Bureau *et al.* 1995). The technique is also being increasingly used in small animals, and preliminary observations suggest that it will be just as useful in the horse (Park *et al.* 1987; Crass *et al.* 1992; Denoix *et al.* 1993; Kaser-Hotz *et al.* 1994; Martinelli *et al.* 1994, 1996; Holcombe *et al.* 1995; Ruohoniemi *et al.* 1997; Kleiter *et al.* 1999; Widmer *et al.* 1999, 2000; Blaik *et al.* 2000).

While many of the early reports of MRI in horses are based on cadaver studies, clinical use of the technique is currently being undertaken at several centres (Mehl *et al.* 1998; Tucker and Sande 2001; Schneider 2002; Schramme 2002; Dyson *et al.* 2003). However, the use of MRI in equine orthopaedics is currently limited because of the expense, availability and logistical problems associated with performing the procedure in large animals. Open and cylindrical MRI scanners designed for human use require the horse to be placed under general anaesthesia in order for the limb to be imaged. This adds

further to the expense of the procedure as well as posing a risk associated with the anaesthesia itself.

Recently, an open MRI scanner¹ designed specifically for imaging the distal limbs of the standing horse has been designed. The first scanner of this type was installed at the Bell Equine Veterinary Clinic and has been in clinical use since June 2002 (Mair and Bolas 2002). Since that time, over 300 horses have been scanned. Although the scanner is designed to enable imaging up to the level of the carpus and tarsus, most of these initial scans have concentrated on the feet. The purpose of this article is to describe the system and scanning procedure, and to discuss some of the applications of this technique. An accompanying report (Kinns and Mair 2005) describes the use of the scanner in evaluating soft tissue damage secondary to deep penetrating wounds of the foot.

Equine MRI limb scanner

The MRI scanner¹ consists of a 'U'-shaped 0.27 tesla permanent magnet, mounted on a frame that is moved using electric motors. The space available between the poles of the magnet is 22 cm across, and the imaging volume is a sphere of approximately 14 cm diameter located at the centre. Movable elements in the floor allow the magnet to be positioned around the foot, and the height is adjustable up to the level of the carpus/tarsus. The system uses Windows NT-based software (also used in human MRI systems) to control the scans and display the images. The system is installed in a purpose-built building incorporating the necessary RF shielding and temperature control (thermostable environment). Radio frequency shielding blocks radio waves and other environmental RF signals that would interfere with the scan. This can be accomplished by installing a copper Faraday cage within the walls, floor and ceiling of the imaging room. Less expensive aluminium screens can also be used.

Scanning procedure

The patient is positioned in specially designed stocks and sedated before bringing the magnet into position. Sedation is

*Author to whom correspondence should be addressed.

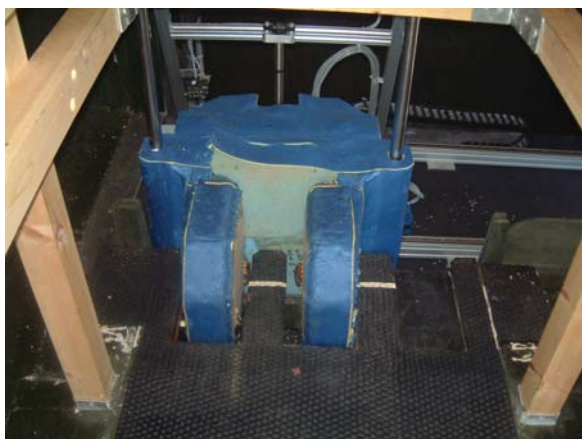


Fig 1: The equine limb MRI scanner showing the magnet fully advanced. The horse stands with its feet approximately on the white lines, and the scanner is advanced around the foot to be imaged.



Fig 2: A horse being scanned. The radiofrequency coil is placed around the area being scanned (in this case the foot).

currently achieved by a combination of romifidine (0.04 mg/kg bwt i.v.), butorphanol (0.02 mg/kg bwt i.v.) and acepromazine (0.02 mg/kg bwt i.v.). ‘Top-up’ sedation is administered as required during the scanning procedure. Following sedation, the receiver radiofrequency coil is fitted around the foot and the magnet moved in around the leg such that the foot is centrally placed (**Figs 1, 2**). Pilot sequences (taking approximately 45 secs) are used to check positioning, correct for any lateral axis deviation, and set the position and angle of subsequent scans.

The current protocol for routine scanning of the foot utilises 3-dimensional (3D) T1- (repetition time [TR] 40, echo delay time [TE] 7, flip angle 60°), multislice T1- (TR 120, TE 7, flip angle 90°), fast spin echo (FSE) T2- (TR 2000, TE 80, flip angle 90°) and FSE STIR (fat-suppressed) (TR 1700, TE 20, flip angle 90°) weighted images in 3 planes. T2*- (TR 200, TE 18, flip angle 40°) weighted images are included in certain situations.

Three-dimensional T1-weighted images taking 32 x 4 mm slices (slice thickness 4.7 mm) are obtained in sagittal and transverse planes to survey the foot. Multislice T1, FSE T2 and FSE STIR images, slice thickness 5 mm, are then taken of the area of interest in 3 planes (sagittal, transverse and frontal planes relative to the hoof-pastern axis). Three mm slices can also be acquired if deemed appropriate. Each image sequence takes between 2.5 mins (T1 multislice) and 4.5 mins (FSE STIR images). Generally, the entire scan protocol takes 60–120 mins (to scan both front or hind feet).

Discussion

Optimisation of the equine limb MRI scanner is still in progress and, to date, it has proved capable of producing diagnostic images of the foot and fetlock of standing horses. Its use in other regions of the distal limbs is currently being evaluated. We believe that this technique could revolutionise the assessment of certain musculoskeletal lesions of the distal limb. The ability to perform MRI in the standing equine patient using the open U-shaped magnet is a considerable advantage

TABLE 1: Appearance of different tissues on T1- and T2-weighted images

Tissue	T1	T2
Medullary cavity/trabecular bone	White	Grey
Cortical bone	Black	Black
Articular cartilage	White	Grey
Tendon/ligament	Black	Black
Fat	White	Grey
Synovium	Grey	White
Synovial fluid	Black	White

over conventional closed magnets that require general anaesthesia. However, the open magnet is, by necessity, of lower field strength than many closed magnets used in human medicine. Lower field strength results in a lower signal-to-noise ratio, and this in turn results in lower resolution or longer imaging times for the same resolution as a higher strength magnet (Rutt and Lee 1996; Tucker and Sande 2001). Imaging time needs to be kept as short as possible because of the risks of movement in the standing horse, but must be long enough to acquire images of adequate resolution. The system described here appears to achieve this goal. Image contrast-to-noise ratio (the ratio of signal intensity difference between 2 tissues and background noise) tends to be higher at lower field strengths (Rothschild *et al.* 1988). Although it is generally accepted that image quality is determined by the signal-to-noise ratio, the contrast-to-noise ratio may be more relevant clinically for distinguishing one tissue type from another (i.e. general lesion detectability) (Rothschild *et al.* 1988).

In addition to permitting use in standing horses, low-field open magnets also have considerable advantages to the veterinary profession in terms of lower initial cost, lower operating costs and no necessity to employ cryogenics (required by super-conducting magnets) (Rutt and Lee 1996; Blaik *et al.* 2000). We believe that this system will allow the application of MRI technology in general equine practice, which would be unlikely with higher-field closed magnets because of their inherently higher cost.

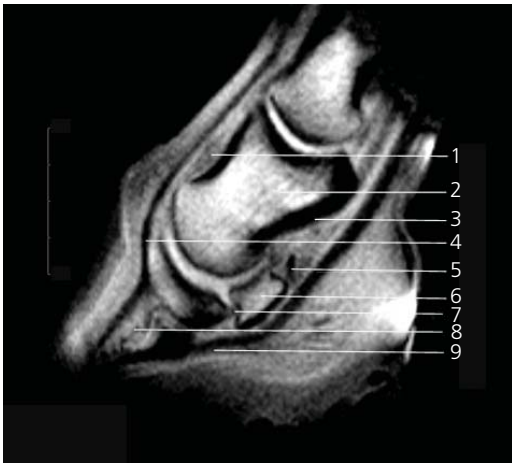


Fig 3: Sagittal T1-weighted image of the foot of a standing normal horse. 1 = Dorsal pouch of the distal interphalangeal joint; 2 = medullary cavity/trabecular bone of middle phalanx; 3 = palmar cortex of middle phalanx; 4 = insertion of dorsal digital extensor tendon onto extensor process of distal phalanx; 5 = collateral (suspensory) ligament of the navicular bone; 6 = medullary cavity of navicular bone; 7 = distal sesamoid impar ligament; 8 = medullary cavity/trabecular bone of middle phalanx; 9 = site of insertion of the deep digital flexor tendon onto the distal phalanx.

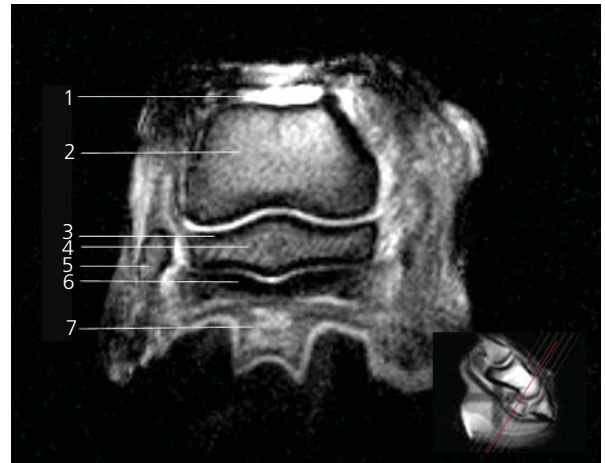


Fig 4: Transverse oblique T2-weighted image of the foot of a standing normal horse. The pilot sequence (inset) shows the position of the slice. 1 = Dorsal pouch of the distal interphalangeal joint; 2 = medullary cavity/trabecular bone of middle phalanx; 3 = cortical bone of the articular surface of the navicular bone; 4 = medullary cavity of navicular bone; 5 = ungular cartilage; 6 = deep digital flexor tendon; 7 = digital cushion (cuneal part).

MRI has many advantages over other conventional imaging techniques, including radiography, ultrasonography, nuclear scintigraphy and computed tomography (CT). MRI does not use ionising radiation and provides multiplanar, 3D imaging capabilities. Both bone and soft tissues can be imaged simultaneously. In addition, MRI allows assessment of physiological differences between normal and abnormal tissues by utilisation of various imaging sequences. Although CT can be used to evaluate bone and soft tissues, soft tissue contrast is inferior to MRI (Whitton *et al.* 1998; Tietje *et al.* 2001).

Interpretation of MR images requires knowledge of MR physics, normal anatomy and characteristic findings in abnormal tissues (Chaffin *et al.* 1997). For example, each examination of the front or hind feet will generate over 100 images, and a comprehensive understanding of foot anatomy is required to mentally visualise normal and abnormal structures within 3D space.

The signal intensities seen in images obtained with this system resemble those reported previously for low-field MRI of the equine tarsus (Blaik *et al.* 2000). The appearance of different tissues in the T1- and T2-weighted images are summarised in **Table 1**. Our standard imaging protocol includes 3D T1-weighted sagittal and transverse images, and multislice T1-weighted sagittal, transverse and frontal images, FSE T2-weighted sagittal and transverse images, and FSE STIR-weighted sagittal and transverse images (**Figs 3–5**). The 3D images encompass the whole foot and are used as an initial anatomical screen. Frontal view slices are particularly helpful in the foot to image the distal border of the navicular bone, distal impar ligament and collateral ligaments of the distal interphalangeal joint. The T1-weighted imaging

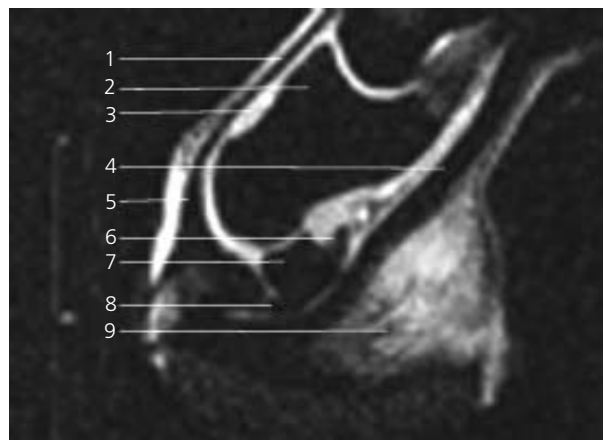


Fig 5: Sagittal STIR image of the foot of a normal horse (cadaver). 1 = Dorsal digital extensor tendon; 2 = medullary cavity/trabecular bone of middle phalanx; 3 = dorsal pouch of distal interphalangeal joint; 4 = deep digital flexor tendon; 5 = medullary cavity/trabecular bone of distal phalanx; 6 = collateral (suspensory) ligament of the navicular bone; 7 = navicular bone; 8 = distal sesamoid impar ligament; 9 = digital cushion.

provides the best anatomical detail, and is considered to be the standard accepted sequence for baseline information of the musculoskeletal system (Kleiter *et al.* 1999). In the foot, the 3D T1-weighted sagittal data set gives a good overview of the bone structure, distal interphalangeal joint and deep digital flexor tendon (DDFT), and the hoof-pastern axis. However, the scan is somewhat sensitive to movement, and may therefore show artefacts that can be mistaken for pathology. The slices are nominally 4–5 mm thick, but the resolution in the slice direction is not perfect, so there may be

some correlation of noise between slices. Therefore, features seen in one slice cannot be confirmed by looking at the adjacent slice in the same way as with multislice images. The 3D T1-weighted transverse images are identical to the sagittal data set, apart from being in transverse orientation. In the foot, the slices are cut perpendicular to the hoof-pastern axis. The view is targeted at the distal interphalangeal joint, but also clearly shows the proximal interphalangeal joint, middle and distal phalanges, navicular bone and DDFT. The multislice T1-weighted transverse sequence collects 5 slices independently of each other; adjacent slices can therefore be compared to each other to confirm that a feature is not an artefact due to noise. In the foot, images are routinely taken perpendicular to the DDFT in the area of interest. These images are particularly useful to identify DDFT damage, which appears as areas of white or grey (high-intensity) signal within the normally black (low-intensity signal) tendon. Tendon damage may also show as thinning and/or a generalised grey appearance through the entire tendon lobe. A poor image to signal noise can mimic these findings, so they need to be interpreted with caution and should be confirmed in at least 2 separate scan planes.

T2-weighted images are particularly useful for evaluating synovial structures. Synovial fluid has a high signal intensity, which appears bright white on the image (Fig 4). T2-weighted images have less resolution than T1-weighted images, and have a grainier appearance. The TE of T2-weighted images is longer than T1-weighted images, and there is therefore a lower signal-to-noise ratio, which results in a more grainy image; they are therefore less useful for studying fine anatomical features. The increase in tissue water that occurs in many disease states results in more mobile hydrogen protons, and this results in longer T2 relaxation times. Therefore, T2-weighted images can be more helpful in identifying disease processes than T1-weighted images. The STIR sequence is a fat-suppression technique that reduces the interference from the fat signal from the medullary cavity of bones, thereby allowing the identification of medullary fluid.

We have shown that MRI of the distal limbs of standing horses is possible using this system. Imaging the feet is technically easy, and both front feet can be imaged in approximately 1–2 h. Movement correction features are currently being evaluated, and these will allow more proximal structures to be assessed. The system has already been used to image the fetlocks, carpus and hocks in a number of horses. Magnetic resonance imaging is not considered to be a screening tool. For optimal results, the imaging should be focused on specific structures or regions determined by previous clinical examinations, including the use of regional analgesia and other imaging modalities where appropriate. Optimal imaging sequences and parameters still need to be determined for the different orthopaedic applications, but it is likely that this system will find an increasing number of applications over the next few years.

Manufacturer's address

¹Hallmarq Veterinary Imaging, Guildford, Surrey, UK.

References

- Blaik, M.A., Hanson, R.R., Kincaid, S.A., Hathcock, J.T., Hudson, J.A. and Baird, D.K. (2000) Low-field magnetic resonance imaging the equine tarsus: normal anatomy. *Vet. Radiol. Ultrasound* **41**, 131-141.
- Buckwalter, K.A. (1996) Magnetic resonance imaging of the knee. *Radiol.* **3**, 99-122.
- Bureau, N., Dussault, R. and Kaplan, P. (1995) MRI of the knee: a simplified approach. *Curr. Probl. Diag. Radiol.* **24**, 1-49.
- Chaffin, M.K., Walker, M.A., McArthur, N.H., Perris, E.E. and Matthews, N.S. (1997) Magnetic resonance imaging of the brain of normal neonatal foals. *Vet. Radiol. Ultrasound* **38**, 102-111.
- Crass, J.R., Genovese, R.L., Render, J.A. and Bellon, E.M. (1992) Magnetic resonance, ultrasound and histopathologic correlation of acute and healing equine tendon injuries. *Vet. Radiol. Ultrasound* **33**, 206-216.
- Denoux, J.-M., Crevier, N., Roger, B. and Lebas, J.-F. (1993) Magnetic resonance imaging of the equine foot. *Vet. Radiol. Ultrasound* **34**, 405-411.
- Dyson, S., Murray, R., Schramme, M. and Branch, M. (2003) Magnetic resonance imaging of the equine foot: 15 horses. *Equine vet. J.* **35**, 18-26.
- Holcombe, S.J., Bertone, A.L., Biller, D.S. and Haider, V. (1995) Magnetic resonance imaging of the equine stifle. *Vet. Radiol. Ultrasound* **36**, 119-125.
- Kaser-Hotz, B., Sartoretti-Scheffer, S. and Weiss, R. (1994) Computed tomography and magnetic resonance imaging of the normal equine carpus. *Vet. Radiol. Ultrasound* **35**, 457-461.
- Kinns, J. and Mair, T.S. (2005) Use of magnetic resonance imaging to assess soft tissue damage in the foot following penetrating injury in 3 horses. *Equine vet. Educ.* **17**, 69-73.
- Kleiter, M., Kneissl, S., Stanek, C., Mayrhofer, E., Baulain, U. and Deegen, E. (1999) Evaluation of magnetic resonance imaging techniques in the equine digit. *Vet. Radiol. Ultrasound* **40**, 15-22.
- Kraft, S.L. and Gavin, P. (2001) Physical principles and technical considerations for equine computed tomography and magnetic resonance imaging. *Vet. Clin. N. Am.: Equine Pract.* **17**, 115-130.
- Mair, T.S. and Bolas, N.M. (2002) MRI of the distal limbs in the standing sedated horse. In: *Proceedings of the 41st Congress of the British Equine Veterinary Association*, Equine Veterinary Journal Ltd., Newmarket. p 206.
- Martinelli, M.J., Baker, G.J., Clarkson, R.B., Eurell, J.C. and Pijanowski, G.J. (1994) Equine metacarpophalangeal joint: correlation between anatomy and magnetic resonance imaging. *Vet. Surg.* **23**, 425.
- Martinelli, M.J., Baker, G.J., Clarkson, R.B., Eurell, J.C., Pijanowski, G.J. and Kuriashkin, I.V. (1996) Magnetic resonance imaging of degenerative joint disease in a horse: a comparison to other diagnostic techniques. *Equine vet. J.* **28**, 410-415.
- Mehl, M.L., Tucker, R.L., Ragle, C.A. and Schneider, R.K. (1998) The use of MRI in the diagnosis of equine limb disorders. *Equine Pract.* **20**, 14-17.
- Park, R.D., Nelson, T.R. and Hoopes, P.J. (1987) Magnetic resonance imaging of the normal equine digit and metacarpophalangeal joint. *Vet. Radiol.* **28**, 105-116.
- Rothschild, P.A., Winkler, M.L., Gronemeyer, D.H.W., Kaufman, L. and D'Amour, P. (1988) Midfield and low-field magnetic resonance imaging of the spine. *Top. Magn. Reson. Imag.* **1**, 11-23.
- Ruohoniemi, M., Karkkainen, M. and Tervahartiala, P. (1997) Evaluation of the variably ossified collateral cartilages of the distal phalanx and adjacent anatomical structures in the Finnhorse with computed tomography and magnetic resonance imaging. *Vet.*

- Radiol. Ultrasound* **38**, 344-351.
- Rutt, B.K. and Lee, D.H. (1996) The impact of field strength on image quality in MRI. *J. Magn. Resonance Imag.* **1**, 57-62.
- Schneider, R.K. (2002) Magnetic resonance imaging (MRI): what have we learned? In: *Proceedings of the 12th Annual Veterinary Symposium of the American College of Veterinary Surgeons*, American College of Veterinary Surgeons, San Diego. pp 75-76.
- Schramme, M.C. (2002) Radiology, ultrasonography, scintigraphy of the foot. In: *Proceedings of the 12th Annual Veterinary Symposium of the American College of Veterinary Surgeons*, American College of Veterinary Surgeons, San Diego. pp 70-74.
- Tietje, S., Nowak, M., Petzoldt, S. and Weiler, H. (2001) Computed tomographic evaluation of the distal aspect of the deep digital flexor tendon (DDFT) in horses. *Pferdheilkunde* **17**, 21-29.
- Tucker, R.L. and Sande, R.D. (2001) Computed tomography and magnetic resonance imaging in equine musculoskeletal conditions. *Vet. Clin. N. Am.: Equine Pract.* **17**, 145-157.
- Whitton, R. C., Buckley, C., Donovan, T., Wales, A.D. and Dennis, R (1998) The diagnosis of lameness associated with distal limb pathology in a horse: comparison of radiography, computed radiography and magnetic resonance imaging. *Vet. J.* **155**, 223-229.
- Widmer, W.R., Buckwalter, K.A., Hill, M.A., Fessler, J.F. and Ivancevich, S. (1999) A technique for magnetic resonance imaging of equine cadaver specimens. *Vet. Radiol. Ultrasound* **40**, 10-14.
- Widmer, W.R., Buckwalter, K.A., Fessler, J.F., Hill, M.A., Van Sickle, D.C. and Ivancevich, S. (2000) Use of radiography, computed tomography, and magnetic resonance imaging for evaluation of navicular syndrome in the horse. *Vet. Radiol. Ultrasound* **41**, 108-116.